

Data and text mining

Supervised graph co-contrastive learning for drug–target interaction prediction

Yang Li ¹, Guanyu Qiao¹, Xin Gao ² and Guohua Wang ^{1,*}

¹College of information and Computer Engineering, Northeast Forestry University, Harbin 150004, China and ²Computer, Electrical and Mathematical Science and Engineering Division, King Abdullah University of Science and Technology, Mathematical and Computer Sciences and Engineering, Thuwal 23955, Kingdom of Saudi Arabia

*To whom correspondence should be addressed.

Associate Editor: Zhiyong Lu

Received on November 2, 2021; revised on February 5, 2022; editorial decision on March 12, 2022; accepted on March 20, 2022

Abstract

Motivation: Identification of Drug–Target Interactions (DTIs) is an essential step in drug discovery and repositioning. DTI prediction based on biological experiments is time-consuming and expensive. In recent years, graph learning-based methods have aroused widespread interest and shown certain advantages on this task, where the DTI prediction is often modeled as a binary classification problem of the nodes composed of drug and protein pairs (DPPs). Nevertheless, in many real applications, labeled data are very limited and expensive to obtain. With only a few thousand labeled data, models could hardly recognize comprehensive patterns of DPP node representations, and are unable to capture enough commonsense knowledge, which is required in DTI prediction. Supervised contrastive learning gives an aligned representation of DPP node representations with the same class label. In embedding space, DPP node representations with the same label are pulled together, and those with different labels are pushed apart.

Results: We propose an end-to-end supervised graph co-contrastive learning model for DTI prediction directly from heterogeneous networks. By contrasting the topology structures and semantic features of the drug–protein-pair network, as well as the new selection strategy of positive and negative samples, SGCL-DTI generates a contrastive loss to guide the model optimization in a supervised manner. Comprehensive experiments on three public datasets demonstrate that our model outperforms the SOTA methods significantly on the task of DTI prediction, especially in the case of cold start. Furthermore, SGCL-DTI provides a new research perspective of contrastive learning for DTI prediction.

Availability and implementation: The research shows that this method has certain applicability in the discovery of drugs, the identification of drug–target pairs and so on.

Contact: ghwang@nefu.edu.cn

1 Introduction

Drug targets are proteins that can be targeted by drugs and produce effects in cells. The identification of interactions between drugs and protein targets is not only an essential step in drug discovery (Feng *et al.*, 2017), but also provides guidance toward drug repositioning, multi-drug pharmacology, drug resistance (Xue *et al.*, 2018) and side effect prediction (Mongia and Majumdar, 2020). However, it is time consuming and expensive to determine drug–target interactions (DTIs) by biological experiments.

In order to speed up drug discovery, researchers have been exploring computational methods to identify DTIs. Existing methods of DTI prediction can be classified into three categories: ligand-based (Keiser *et al.*, 2007), docking-based (Shaikh *et al.*, 2016) and machine learning-based approaches (Wen *et al.*, 2017). In addition to the widely used traditional algorithms, a remarkable trend is to approach DTIs

from a network perspective. Graph representation learning models such as graph convolutional network (GCN) (Kipf and Welling, 2016) and graph attention network (GAT) (Velickovi *et al.*, 2017) have been used to learn from various types of homogeneous or heterogeneous network information for DTI prediction (Sun *et al.*, 2020). Most existing methods are mainly divided into two independent steps: first to extract the representation vectors of drugs and proteins, and second to apply a deep neural network to predict the final label based on the representation. To the best of our knowledge, there are only few end-to-end models to directly predict the interactions between drugs and proteins from many heterogeneous networks.

In addition to the early computational DTI prediction methods, such as ligand-based (González-Díaz *et al.*, 2011) and docking-based methods (Cheng *et al.*, 2012; Meng *et al.*, 2017), machine learning methods have attracted great attention, as they enable large scale testing of candidates in a relatively short time (Gao *et al.*,

2018; Peng et al., 2020). A key idea behind these methods is the hypothesis of ‘guilt-by-association’, which means that similar drugs may have similar targets and vice versa (Luo et al., 2017). Based on this assumption, machine learning models such as random forest (RF), decision tree (DT) and support vector machine (SVM) are widely used as classifiers to predict whether a DTI is present or not.

On the other hand, some advanced machine learning methods have been proposed to integrate external information for DTI prediction. Yamanishi et al. (2010) developed a bipartite graph model where the chemical and genomic spaces as well as the drug–protein interaction network are integrated into a pharmacological space. Xia et al. (2010) proposed a semi-supervised learning method, Laplacian regularized least square (LapRLS), to utilize both the small amount of available labeled data and the abundant unlabeled data together in order to give the maximum generalization ability from the chemical and genomic spaces. At the same time, pharmacological or phenotypic information, such as side-effects (Mizutani et al., 2012), transcriptional response data (Iorio et al., 2010), drug–disease associations (Wang et al., 2014), public gene expression data (Sirota et al., 2011) and functional data have been incorporated in DTI to provide diverse information and a multi-view perspective for predicting novel DTIs. Luo et al. (2017) proposed a network integration pipeline DTINet to integrate heterogeneous data sources (e.g. drugs, proteins, diseases and side-effects). Most of the above methods rely on traditional machine learning, ignoring the topology information of drugs and proteins, and unable to learn the deep interactions between them.

In recent years, with the great success of deep learning in various fields of bioinformatics, network representation learning methods, which can learn rich topological information and the complex interaction between heterogeneous data, have been used in DTI prediction (Sun et al., 2020; Zeng et al., 2020). Peng et al. (2020) proposed a learning-based method DTI-CNN for DTI prediction that learns low-dimensional vector representations of features from heterogeneous networks. DTI-CNN takes the concatenate representation vector of drugs and proteins as input, and adopts convolution neural networks (CNN) as the classification model. Nevertheless, DTI-CNN ignores the interactions between drug and protein pairs (DPPs) in the modeling and learning process. To incorporate associations between DPPs into DTI modeling (Zhao et al., 2021) built a DPP network based on multiple drugs and proteins in which DPPs are the nodes and the associations between DPPs are the edges of the network. Then they proposed a model GCN-DTI for DTI identification. The model first uses a GCN to learn the representation for each DPP, and applies a deep neural network to predict the final label based on the representation. Although this method noticed that neighbor DPPs may have an influence on each other, it ignored the semantic feature of the DPP network. At the same time, whether the noise in the graph can be removed, or whether the model can learn more effective representation from limited labeled data, is still unresolved.

Nevertheless, in many real applications such as DTI prediction, labeled data is limited and expensive to obtain. Recently, self-supervised contrastive learning has attracted considerable attention in many graph representation learning tasks. Current work mainly focus on designing different graph augmentation strategies to produce two representations of the same node and leverage a contrastive learning loss to maximize agreement between them, while minimizing the similarity between ‘other negative samples’ (You et al., 2020). GraphCL (Hafidi et al., 2020) learns node embeddings by maximizing agreement/similarity between the representations of two randomly perturbed versions of the same node’s local subgraph. You et al. (2020) designed four types of graph data augmentation (node dropping, edge perturbation, attribute masking and subgraph) and studied the influence of various combinations of data argumentation in different tasks. Zhu et al. (2020) combined many kinds of prior knowledge to enhance interference to unimportant nodes and edges, and retain the internal structure and attribute information of the graph. In the field of bioinformatics, graph contrastive learning is applied to DDI prediction, comparing the original graph representation with the processed graph representation (Wang et al., 2021b).

At the same time, Ciortan and DeFrance (2021) used two encoders to randomly mask the sequences in the scRNA-seq and conducted contrastive learning on the augmented data. However, little effort has been made to fully leverage valuable *label information* to supervise the construction of *effective positive and negative pairs* in the contrastive loss.

Probably, most relevant work is the model of Wang et al. (2021a) which uses two views of a heterogeneous information network (network schema and meta-path views) to learn node embeddings. Then the cross-view contrastive learning is proposed to extract the positive and negative embeddings from two views. The key difference is that we try to utilize the valuable supervision information, and seek the commonalities between examples of each class and contrast them with examples from other classes (Gunel et al., 2021; Khosla et al., 2020). Through the contrast of the topology structures and semantic features of the DPP network, the two views collaboratively supervise each other and guide the model optimization in a supervised manner.

As illustrated in Figure 1, motivated by the intuition that the similarity between first-order neighbor nodes in one class is higher, we propose an end-to-end Supervised Graph Co-contrastive Learning model for DTI prediction, namely SGCL-DTI. Specifically, SGCL-DTI first learns low-dimensional representations of drugs and proteins from heterogeneous networks through a meta-path guided graph encoder. After that, a topology graph and a semantic graph for drug–protein pair (DPP) nodes are constructed, respectively. Different from previous contrastive learning which contrasts the original network and the corrupted network, we optimize the final prediction objective function through the co-contrastive learning of the two DPP networks, by maximizing the similarity between first-order neighbors in one class and contrasting them with nodes in other classes (Gunel et al., 2021). We conduct comprehensive experiments on three public datasets and show that our model outperforms the SOTA methods significantly.

The key contributions of this article can be summarized as follows:

- We propose a supervised graph co-contrastive learning model for the task of DTI prediction. Through contrastive learning of multiple views while incorporating the supervision information, SGCL-DTI significantly outperforms the SOTA methods over all the datasets. To the best of our knowledge, this is the first attempt that contrasts topology structures and semantic features of the same graph in a supervised manner.
- We thoroughly design and conduct comprehensive experiments to prove the effectiveness of different components in our model, and also analyze different positive and negative sample selection strategies in contrastive learning on this task.
- SGCL-DTI is a generic end-to-end graph representation learning framework and can be easily extended to other applications.

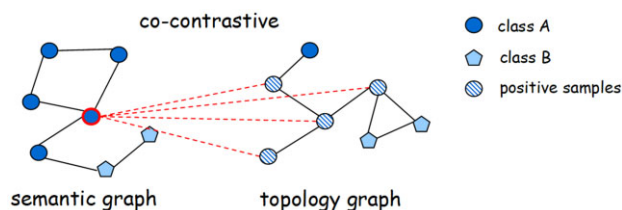


Fig. 1. An example of supervised graph co-contrastive learning. Nodes of different shapes indicate that they have different class labels (class A and class B). Class A represents a verified interaction between the drug and the target in this DPP, while class B represents no interaction between the drug and the target in the DPP. The node in the circle with bold border is a target node in the semantic graph. Its corresponding node and the first-order neighbors of the same class from the topology graph are selected as its positive samples and connected to it with the dashed lines

2 Materials and methods

In this section, we present our model for DTI prediction and explain the motivation and the key idea behind our model. The architecture of our proposed model, SGCL-DTI, is shown in Figure 2. It consists of four components: Heterogeneous Information Network Construction, Meta-path-based Graph Encoder, DPP Network Representation Learning and Supervised Co-contrastive Optimization. First, to model different types of entities and their complex relationships, we utilize a heterogeneous information network to depict drugs, proteins and corresponding heterogeneous relations among them. Next, a meta-path-based graph encoder with the attention mechanism is used to learn the representation of drug and protein nodes from the heterogeneous information network. Then, the topology network and the semantic network of DPPs are constructed and learned, where each DPP node is the concatenation of a drug and a protein representation. In this way, we can learn not only the relationship between DPP nodes, but also the interaction within drug-protein pairs. Finally, a novel contrastive optimization module is used to generate a collaborative contrastive loss of the two views, and guide the model optimization in a supervised manner.

2.1 Heterogeneous information network construction

A *Heterogeneous Information Network* $\mathcal{G} = (\mathcal{V}, \mathcal{E})$ is a graph where \mathcal{V} is a set of nodes and \mathcal{E} is a set of edges. \mathcal{G} is associated with a node type mapping function $\phi: \mathcal{V} \rightarrow \mathcal{N}$ and an edge type mapping function $\varphi: \mathcal{E} \rightarrow \mathcal{R}$. \mathcal{N} and \mathcal{R} denote sets of object and link types, where $|\mathcal{N} + \mathcal{R}| > 2$.

Inspired by the previous work (Luo et al., 2017), we collect diverse information from the public databases to construct the heterogeneous network for our DTI prediction task, among which there are four drug-related networks (drug-drug relationship network, drug-related disease network, drug and side-effect network and drug-chemical structure similarity network), three protein related networks (protein-related disease network, protein-protein relationship network and protein-sequence similarity network) and one drug-protein interaction network used as our ground-truth. In this study, we model the drug and protein data as an HIN \mathcal{G} . Specifically, the constructed HIN \mathcal{G} includes four entities (i.e. drug, protein, disease and side-effect) and a series of relationships among them.

2.2 Meta-path-based graph encoder

Traditional GCNs can only capture the homogeneous relationships in homogeneous networks, which overlook the rich information among them. To address this issue, meta-paths are used to capture the heterogeneous context information in a heterogeneous graph (Fu et al., 2016; Gong et al., 2020). We learn the representation of

drugs and proteins according to the pre-defined meta-paths with a graph encoder. Considering that different meta-paths may have different influences on the final representation learning of drugs or proteins, we utilize the attention mechanism to fuse the representation of drugs or proteins learned under the guidance of different meta-paths to generate the joint attention representation.

2.2.1 Meta-path selection

A *Meta-path* in \mathcal{G} is defined on a network schema $\mathcal{S} = (\mathcal{N}, \mathcal{R})$ and is denoted as a path in the form of $N_1 \xrightarrow{R_1} N_2 \xrightarrow{R_2} \dots \xrightarrow{R_l} N_{l+1}$, which describes a composite relation $R = R_1 \circ R_2 \circ \dots \circ R_l$ between node types N_1 and N_{l+1} , \circ denotes the composition operator on relations.

Typical meta-paths between two drugs can be defined as follows: drug $\xrightarrow{\text{treat}}$ disease $\xrightarrow{\text{treat}^{-1}}$ drug, which means that two different drugs are related because they can treat the same disease; drug $\xrightarrow{\text{cause}}$ side-effect $\xrightarrow{\text{cause}^{-1}}$ drug, which denotes that two drugs are related in containing chemical components that cause the same side effects. On the other hand, a meta-path between two kinds of proteins can be defined as protein $\xrightarrow{\text{express}}$ disease $\xrightarrow{\text{express}^{-1}}$ protein, which denotes that two kinds of protein are related due to the abnormal expression on the same disease. In total, we induce five meta-paths for drugs and four meta-paths for proteins from \mathcal{G} , as shown in Figure 2.

2.2.2 Meta-path guided GCN

After the appropriate meta-paths are selected, we learn the representations of drugs and proteins based on different meta-paths through GCN. Given an HIN $\mathcal{G} = (\mathcal{V}, \mathcal{E})$ with a group of meta-paths $\mathcal{P} = \{P_1, P_2, \dots, P_M\}$ and the corresponding adjacency matrix $\mathcal{A} = \{A_1, A_2, \dots, A_M\}$ (M represents the number of meta-paths).

First, we use a multi-layer GCN to generate the drug representation based on each meta-path of the drug as follows:

$$\mathbf{z}_{p_i}^{(l)} = \text{ReLU}\left(\mathbf{D}_{p_i}^{-\frac{1}{2}} \tilde{\mathbf{A}}_{p_i} \mathbf{D}_{p_i}^{-\frac{1}{2}} \mathbf{z}_{p_i}^{(l-1)} \mathbf{W}_{p_i}^{(l)}\right) \quad (1)$$

where $\text{ReLU}(x) = \max(0, x)$ is a rectified linear activation function. $\mathbf{z}_{p_i}^{(l)}$ denotes the (l) -Layer representation of drug, in which the subscript i means the i th meta-path of drugs. Specially, $\mathbf{z}^{(0)}$ is the input vector which is initialized from a standard normal distribution. We add an identity matrix \mathbf{I}_{p_i} to the adjacency matrix \mathbf{A}_{p_i} to indicate the node itself, where $\tilde{\mathbf{A}}_{p_i} = \mathbf{A}_{p_i} + \mathbf{I}_{p_i}$. \mathbf{D}_{p_i} is the diagonal matrix of $\tilde{\mathbf{A}}_{p_i}$, $\mathbf{W}_{p_i}^{(l)} \in \mathbb{R}^{d_{in} \times d_{out}}$ is the shared trainable weight matrix for both drugs and proteins at layer l . d_{in} and d_{out} represent the input dimension and output dimension of each layer of GCN respectively.

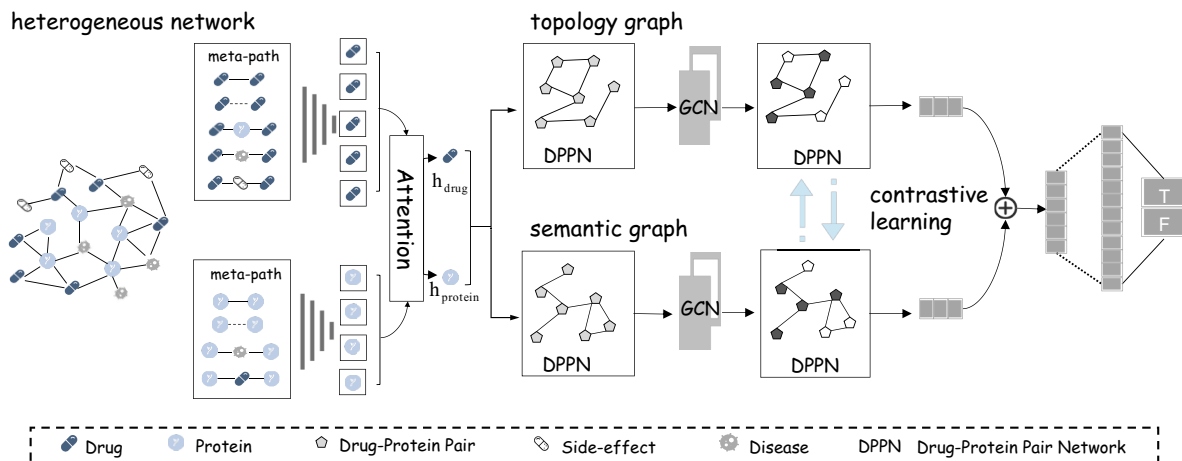


Fig. 2. The overall architecture of the proposed model SGCL-DTI

In order to learn the different influences of different meta-paths for the final representation of drugs, given the corresponding representation of each meta-path of drugs $\mathbf{e}_{p_i} \in \{\mathbf{e}_{p_1}, \mathbf{e}_{p_2}, \dots, \mathbf{e}_{p_{M_d}}\}$, we can learn the attention weights and obtain the final drug representation \mathbf{h}_{drug} as follows:

$$\mathbf{h}_{\text{drug}} = \sum_{i=1}^{M_d} \text{att}(\mathbf{e}_{p_i}) \mathbf{e}_{p_i} \quad (2)$$

$$\alpha_{p_i} = \mathbf{q} \cdot \tanh(\mathbf{W} \cdot \mathbf{e}_{p_i} + \mathbf{b}) \quad (3)$$

where $\mathbf{W} \in \mathbb{R}^{d_i \times d_p}$ is a weight matrix, $\mathbf{b} \in \mathbb{R}^{d_i \times 1}$ is a bias vector and $\mathbf{q} \in \mathbb{R}^{d_i \times 1}$ is a shared attention vector. d_i is the dimension of the attention layer. d_p is the dimension of \mathbf{e}_{p_i} . The obtained weight values are normalized by softmax function as attention scores $\text{att}(\mathbf{e}_{p_i}) = \text{softmax}(\alpha_{p_i})$.

Similarly, we can obtain the protein representation $\mathbf{h}_{\text{protein}}$ based on each meta-path of the proteins.

2.3 DPP network representation learning

To capture the deep and comprehensive relationships between drugs and proteins, we combine each drug p and protein q to form a DPP i through the concatenation. The representation of DPP node i can be represented as $\mathbf{h}_{\text{DPP}}^i = \{\mathbf{h}_{\text{drug}}^p; \mathbf{h}_{\text{protein}}^q\}$. Inspired by a recent study (Wang et al., 2020), we try to construct multi-channel networks for the DPPs. The topology graph models the structural information of DPPs, while the semantic graph learns the semantic information of DPPs.

2.3.1 Topology graph construction

First, we build the topology graph $G_t = (\mathbf{A}_t, \mathbf{X}_{\text{DPP}})$, where $\mathbf{X}_{\text{DPP}} \in \mathbb{R}^{N_{\text{DPP}} \times d_{\text{DPP}}}$ is the representation matrix of all the DPP nodes, N_{DPP} represents the total number of DPPs, d_{DPP} is the dimension of a DPP representation vector. We follow the principle that if two DPPs contain a common drug or a common protein, there is an edge between them. The adjacency matrix $\mathbf{A}_t \in \mathbb{R}^{N_{\text{DPP}} \times N_{\text{DPP}}}$ represents the relationship of edges between nodes in a graph. The value of element in the i th row and the j th column of \mathbf{A}_t equals to 1, meaning that the two DPPs share some common features, and it is 0 in contrary.

2.3.2 Semantic graph construction

We construct the semantic graph of DPPs based on the semantic similarity of learned representations. For each DPP i , we calculate the cosine similarity of the representation between i and other DPPs, and then select the top K nearest DPP nodes as its adjacent nodes (Kipf and Welling, 2016). For example, if DPP j and DPP k are adjacent nodes of DPP i , then we can define in the adjacent matrix \mathbf{A}_s , the element in the i th row and the j th column and the element in the i th row and the k th column to be 1, and 0 otherwise. Therefore, we can construct a semantic graph of DPPs $G_s = (\mathbf{A}_s, \mathbf{X}_{\text{DPP}})$, where \mathbf{A}_s is the adjacency matrix.

2.3.3 DPP network learning

We use two multi-layer GCNs to learn the representation of two DPP networks. Let \mathbf{z}_t and \mathbf{z}_s denote the DPP node representation learned from the topology graph and the semantic graph respectively, the output of the l th layer of GCN models is as follows:

$$\mathbf{z}_t^{(l)} = \text{ReLU}(\tilde{\mathbf{D}}_t^{-\frac{1}{2}} \tilde{\mathbf{A}}_t \tilde{\mathbf{D}}_t^{-\frac{1}{2}} \mathbf{z}_t^{(l-1)} \mathbf{W}_t^{(l)}) \quad (4)$$

$$\mathbf{z}_s^{(l)} = \text{ReLU}(\tilde{\mathbf{D}}_s^{-\frac{1}{2}} \tilde{\mathbf{A}}_s \tilde{\mathbf{D}}_s^{-\frac{1}{2}} \mathbf{z}_s^{(l-1)} \mathbf{W}_s^{(l)}) \quad (5)$$

where $\tilde{\mathbf{A}}_{(\cdot)} = \mathbf{A}_{(\cdot)} + \mathbf{I}_{(\cdot)}$, $\mathbf{I}_{(\cdot)}$ is an identity matrix, $\tilde{\mathbf{D}}_{(\cdot)}$ is the diagonal degree matrix of $\mathbf{A}_{(\cdot)}$ and $\mathbf{W}_{(\cdot)}^{(l)}$ is the weight matrix of the l th layer of GCN.

2.4 Supervised co-contrastive optimization

In this article, we propose a supervised contrastive learning objective to minimize intra-class variance by pulling together examples belonging to the same class and maximize inter-class variance by pushing apart samples from different classes. The supervised contrastive learning (SCL) strategy in SGCL-DTI is similar to the contrastive objectives used in self-supervised graph contrastive learning. The difference is that the contrastive objective is used to supervise the learning of the final prediction task, instead of contrasting different augmented views of examples.

Hence, the objective in SGCL-DTI includes a supervised classification term and a contrastive learning term for DTI prediction. When calculate the contrastive loss, we need to define positive and negative samples. Different from previous work, we propose a new positive sample selection strategy based on the topology network and the semantic network. Specifically, given a DPP node i in the topology network, we not only take its corresponding node j in the semantic network as a positive sample, but also take node j 's first-order neighbor nodes with the same class label as positive samples. We think that first-order neighbor nodes with the same class label are highly correlated. Hence, we can realize the collaborative contrastive learning between the two graphs.

The supervised co-contrastive learning loss of the topology graph $\mathcal{L}_{\text{SCL}}^t$ can be defined as follows:

$$\mathcal{L}_{\text{SCL}}^t = - \sum_{i=1}^{N_{\text{DPP}}} \log \frac{\sum_{j \in \mathbb{P}_i} \exp(\text{sim}(\mathbf{z}_t^i, \mathbf{z}_t^j) / \tau)}{\sum_{k \in \{\mathbb{P}_i \cup \mathbb{N}_i\}} \exp(\text{sim}(\mathbf{z}_t^i, \mathbf{z}_t^k) / \tau)} \quad (6)$$

where \mathbb{P}_i is the set of positive samples of DPP node i ($i \in G_t$), which is composed of node j ($j \in G_s$) and node j 's first-order neighbor nodes with the same class label. \mathbb{N}_i is the set of negative samples of node i , representing all the other nodes not in \mathbb{P}_i . τ is an adjustable scalar temperature parameter. Similarly, we can obtain the supervised co-contrastive learning loss of the semantic graph $\mathcal{L}_{\text{SCL}}^s$.

We model the task of DTI prediction as a binary classification problem, that is to predict whether there is an interaction between a DPP pair x_i . The loss function of classification can be defined as:

$$\mathcal{L}_{\text{CE}} = - \sum_{i=1}^{N_{\text{DPP}}} [y_i \log \pi(x_i) + (1 - y_i) \log (1 - \pi(x_i))] \quad (7)$$

where $\pi(x) = P(Y = 1|x)$ and $y \in \{0, 1\}$.

Finally, the optimization objective of our model consists of three parts: the classification loss, the contrastive loss and the L2 regularization term $R(\Theta)$:

$$\mathcal{L} = \mathcal{L}_{\text{CE}} + \lambda \mathcal{L}_{\text{SCL}}^t + (1 - \lambda) \mathcal{L}_{\text{SCL}}^s + \gamma R(\Theta) \quad (8)$$

where $R(\Theta) = \sum (\Theta)^2$ (i.e. the sum of the squared weight values), Θ represents all the trainable model parameters.

3 Results

In this section, we first introduce the datasets, comparison methods and evaluation metrics used in the experiment. Then, we conduct experiments to answer the following questions: (i) Is it feasible and effective to predict the DTIs based on the proposed SGCL-DTI? (ii) Is it useful to incorporate supervised contrastive learning and co-contrastive learning into the framework? (iii) Is our strategy of selecting positive and negative samples effective comparing to others? (iv) What is the effect of our method for special cases such as cold-start DPPs?

3.1 Experimental setup

3.1.1 Dataset

To evaluate the performance of the end-to-end heterogeneous graph representation learning-based framework for DTI prediction, we test our model on three widely used datasets in previous studies,

namely, Zheng's DTIdata, Luo's DTIdata and Yamanishi's DTIdata. These three datasets belong to large, medium and small datasets in scale.

- **Zheng's DTIdata** (Zheng *et al.*, 2018): There were 11 819 experimentally verified interactions between 1094 drugs and 1556 target proteins in the dataset. In addition, besides drugs and targets it also contains four kinds of heterogeneous information: drug substitute, chemical structure, drug side-effect and gene ontology.
- **Luo's DTIdata** (Luo *et al.*, 2017): There are four types of nodes (drug, protein, disease and side-effect) and eight types of interactions constructing totally six heterogeneous interaction types (drug–drug interaction, drug–protein interaction, drug–disease interaction, drug–side effect interaction, protein–protein interaction and protein–disease interaction) and two similarity networks (pharmacochemical structure similarity network and protein sequences similarity network), which covers 12 015 nodes and 1 894 854 edges in total.
- **Yamanishi's DTIdata** (Yamanishi *et al.*, 2010): There are four sub-datasets [nuclear receptor (NR), G-protein-coupled receptor (GPCR), ion channels (IC) and enzyme] including 1481 drugs and 1408 proteins, with a total of 9880 DTIs. Besides, each sub-dataset contains a drug–drug similarity network and a protein–protein similarity network.

3.1.2 Baselines

For comparison, we use the following competitive methods for DTI prediction as baselines:

- **DTINet** (Luo *et al.*, 2017): A novel network integration pipeline for DTI prediction. DTINet learns low-dimensional feature vectors of drugs and targets across multiple networks, and then finds an optimal projection from the drug space onto the target space and predicts the interactions.
- **GCN-DTI** (Zhao *et al.*, 2021): GCN for DTI prediction. To incorporate the association within a drug–protein pair, GCN-DTI constructs a DPP network based on multi-drugs and proteins, which takes DPP as the node and the association between DPP as the edge of the network. On this basis, the model uses a graph convolution network to learn the characteristics of each DPP, and the final label is predicted by using a deep neural network.
- **IMCHGAN** (Li *et al.*, 2021): Inductive Matrix Completion with Heterogeneous GAT. IMCHGAN proposes a two-level GAT to learn drug and target latent feature representations from the DTI heterogeneous network separately, and adopts the inductive matrix completion to predict the DTIs.

- **EEG-DTI** (Peng *et al.*, 2021): An end-to-end learning framework based on heterogeneous GCNs for DTI prediction. EEG-DTI constructs a heterogeneous network by combining eight types of biological networks, and using the inner product method to calculate the interaction score between drugs and targets based on the learned low-dimensional representations.

3.1.3 Experiment settings

For all the comparison methods mentioned above, we carry out experiments on the same dataset with our model and follow the parameter settings in their papers. For our model, the number of GCN layers is 2, the dimensions of the two hidden layers are 256 and 128, respectively. We use an Adam algorithm to train the model for 1000 iterations with early stop. The learning rate is set to be $1e-4$ with a weight decay rate of $1e-10$, the dropout rate is 0.5. The temperature parameter τ is set to 0.8. For all the experiments, we perform 5-fold cross-validation. We first randomly divide the positive DPPs (there is an interaction between the drug and the target) into five subsets. At the same time, we randomly select DPPs without interaction as counterexamples, so that the positive and negative examples can be balanced in the process of model training. In each run, we use four subsets as training data and the fifth subset for testing. This is repeated five times and we report the average performance.

3.2 Experiment results

3.2.1 Comparison with baselines

We compare our model and the baselines on the task of DTI prediction, the AUROC and AUPR results are shown in Table 1. We can draw the following conclusions: (i) the methods based on graph neural networks (GCN-DTI, IMCHGAN, EEG-DTI and SGCL-DTI) generally perform better than the deep learning method DTINet, which shows that graph neural network has advantages in learning the interactions from heterogeneous networks. According to this result, we analyze that the graph neural networks learning to update the central node by aggregating the neighbor information of nodes, so that the model can learn the interactions between nodes and more effective node representations, and finally improving the node classification task. (ii) The end-to-end models (IMCHGAN, EEG-DTI and SGCL-DTI) work better on most datasets, especially on large ones. Our model outperforms the other two end-to-end approaches. The reason may be that we use a supervised co-contrastive learning framework to restrict graph representation learning from semantic graph and topology graph respectively, and maximizing the similarity between first-order neighbors in one class and contrasting them with nodes in other classes, so that the model has good generalization performance. (iii) Our model SGCL-DTI achieves the best performance in all the datasets. Compared with the other competitive baselines, SGCL-DTI improves at least 2% in terms of AUROC and AUPR. The above experimental results demonstrate that our supervised graph co-contrastive learning method is effective for DTI prediction.

Table 1. Comparison of results between our model and the baselines

Method	Luo's DTIdata		Zheng's DTIdata		Yamanishi's DTIdata							
	AUROC	AUPR	AUROC	AUPR	GPCR		Enzyme		IC		NR	
					AUROC	AUPR	AUROC	AUPR	AUROC	AUPR	AUROC	AUPR
DTINet	0.8798	0.9063	0.8898	0.9006	0.8448	0.8871	0.9239	0.9418	0.8353	0.8726	0.8712	0.8386
GCN-DTI	0.9183	0.8975	0.9222	0.9146	0.9299	0.9183	0.9757	0.9659	0.9773	0.9752	0.9321	0.9222
IMCHGAN	0.9568	0.9586	0.9485	0.9398	0.9485	0.9479	0.9658	0.9400	0.9542	0.9471	0.9324	0.8951
EEG-DTI	0.9548	0.9643	0.9425	0.9415	0.9642	0.9631	0.9833	0.9726	0.9841	0.9759	0.9012	0.9122
SGCL-DTI	0.9771	0.9768	0.9684	0.9680	0.9741	0.9812	0.9892	0.9895	0.9857	0.9852	0.9438	0.9578

Bold is to show the better results in this experiment.

Table 2. Results of ablation study on Luo's DTI data

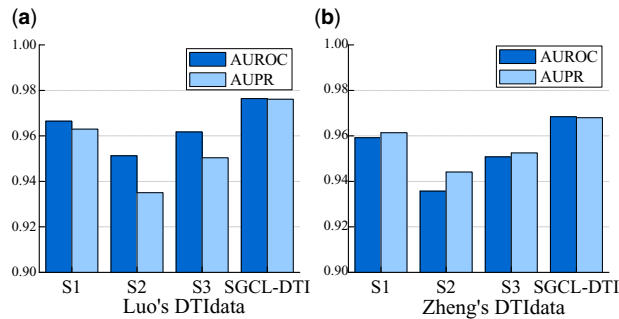
Method	AUROC	AUPR
Without contrastive learning	0.9602	0.9648
Without semantic graph	0.8916	0.9089
Without topology graph	0.9012	0.9193
Without co-contrastive learning	0.8851	0.8989
SGCL-DTI	0.9771	0.9768

Bold is to show the better results in this experiment.

Table 3. Results of ablation study on Zheng's DTI data

Method	AUROC	AUPR
Without contrastive learning	0.9391	0.9389
Without semantic graph	0.8651	0.8525
Without topology graph	0.8902	0.8847
Without co-contrastive learning	0.8711	0.8869
SGCL-DTI	0.9684	0.9680

Bold is to show the better results in this experiment.

**Fig. 3.** Comparison of selection strategy of positive and negative samples

In summary, we guess that our model works well because the nodes are updated in two views, and the choice of contrastive learning strategy also improves the results. Next, we will test our conjecture through experiments.

3.2.2 Ablation study

To test the effectiveness of different components in our model, we conduct ablation study on the two largest datasets. Specifically, we denote our method as the full model SGCL-DTI and perform the leave-one-out validation on each part of the model. The model 'Without contrastive learning' denotes our model which uses meta-path and multi-view GCN, but without contrastive learning. The model 'Without semantic graph' denotes our model using only the topology graph and contrastive learning within one graph. The model 'Without topology graph' denotes our model using only the semantic graph and contrastive learning within one graph. The model 'Without co-contrastive learning' denotes our model that removes both contrast learning and multi-view graph learning.

From Tables 2 and 3, we can draw the following conclusions: (i) either only using the topology graph or the semantic graph, the results decrease by about 8% comparing to the full model. This result shows that multi-view is effective for DTI prediction. (ii) Comparing the results of 'Without contrastive learning' and SGCL-DTI, the contrastive learning strategy improves the results on the two datasets by nearly 2%. (iii) When we remove co-contrastive learning cross multiple graphs 'Without co-contrastive learning', the result is the worst.

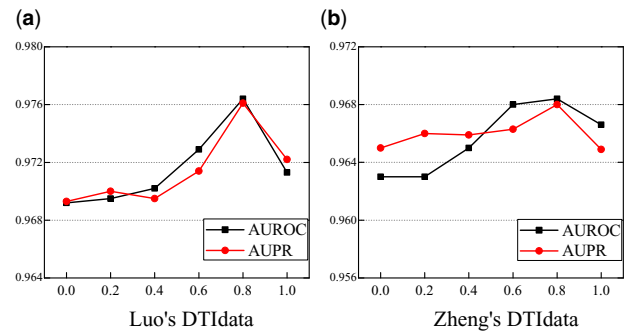
3.2.3 Selection strategy of positive and negative samples

In contrastive learning, the selection strategy of positive and negative samples will affect the final result. Therefore, in this part, we will

Table 4. Results of cold start analysis in Luo's DTI data and Zheng's DTI data, where N represents the number of interactions, and C represents the number of cold start nodes

Method	Luo's DTI data			Zheng's DTI data		
	$N=0$ $C=37$	$N \leq 3$ $C=503$	$N \leq 5$ $C=1074$	$N \leq 3$ $C=98$	$N \leq 5$ $C=378$	$N \leq 10$ $C=2245$
GCN-DTI	0.7837	0.7912	0.8007	0.8163	0.7883	0.7866
IMCHGAN	0.8618	0.8767	0.8916	0.8163	0.8571	0.8094
EEG-DTI	0.8649	0.8767	0.8585	0.8371	0.8536	0.9070
SGCL-DTI	0.8919	0.9284	0.9283	0.8470	0.8730	0.8837

Bold is to show the better results in this experiment.

**Fig. 4.** Results of parameter sensitivity analysis with different λ **Table 5.** Results of different initialization strategies in Luo's DTI data

Method	Luo's strategy		SGCL-DTI	
	AUROC	AUPR	AUROC	AUPR
Fold 1	0.9782	0.9795	0.9807	0.9787
Fold 2	0.9474	0.9548	0.9664	0.9754
Fold 3	0.9658	0.9624	0.9727	0.9758
Fold 4	0.9798	0.9674	0.9804	0.9793
Fold 5	0.9779	0.9659	0.9857	0.9746
Average	0.9698	0.9660	0.9771	0.9768

compare several strategies widely used in previous work. Given that we have two DPP networks G_t and G_s , and two augmented views \tilde{G}_t and \tilde{G}_s obtained by edge perturbation and attribute masking:

- **Strategy S1:** Using a DPP node i 's corresponding node j in the opposite network as the positive sample.
- **Strategy S2:** Using a DPP node i 's corresponding node j in its augmented view as the positive sample.
- **Strategy S3:** For a DPP node i in one augmented view, using its corresponding node j in another augmented view as the positive sample.

From Figure 3, we find that the contrastive learning methods between the topology graph and the semantic graph (S1 and our method SGCL-DTI), outperform the contrastive learning between one graph and its augmented view (S2 and S3). Furthermore, our method has achieved the best results due to the introduction of supervision information and co-contrastive learning.

3.2.4 Cold start analysis

Previous experiments can prove that the supervised graph co-contrastive learning can greatly improve the results of DTI

Table 6. Results of positive and negative examples with different proportions in Luo's DTI data

Proportion	1:1		1:5		1:10	
	AUROC	AUPR	AUROC	AUPR	AUROC	AUPR
Fold 1	0.9807	0.9787	0.9767	0.9560	0.9838	0.9456
Fold 2	0.9664	0.9754	0.9634	0.9367	0.9716	0.9340
Fold 3	0.9727	0.9758	0.9807	0.9531	0.9852	0.9432
Fold 4	0.9804	0.9793	0.9843	0.9602	0.9897	0.9568
Fold 5	0.9857	0.9746	0.9903	0.9690	0.9943	0.9611
Average	0.9771	0.9768	0.9791	0.9550	0.9849	0.9481

prediction. However, when there is little information about the interaction between a drug and a protein node, the learning ability of most models may decrease greatly. This is a very common cold start scenario in real-world applications. Therefore, we conduct the cold start analysis. We select the DPP nodes with less than or equal to 0, 3, 5 relationships in Luo's DTI data, and the DPP nodes with less than or equal to 3, 5, 10 relationships in Zheng's DTI data as cold start nodes, respectively. The results in Table 4 show that our model still outperforms other baseline methods under cold start conditions, and, interestingly, the improvement is even more obvious.

3.2.5 Parameter sensitivity analysis

Next, we conduct the parameter sensitivity experiment of our model. First of all, we vary the value of the coefficient λ in the loss function (Equation 8), to explore the influence of the contrastive learning loss on the model. From Figure 4, we try the following values of $\lambda = \{0, 0.2, 0.4, 0.6, 0.8, 1\}$, and find that the performance improves when λ increases. The best results are achieved when λ is close to 0.8.

Second, we test different initialization strategies to drugs and targets embedding. We compare our model using our initialization method with the setting of initialization method in Luo's paper (Luo et al., 2017). In Luo's paper, the initialization vectors of drugs and proteins are 100-dimensional and 400-dimensional feature vectors obtained from feature engineering. The results of 5-fold cross validation in Table 5 demonstrated that both initialization methods perform well in our model. Although we randomly assigned initial values to drugs and targets based on the normal distribution, in our model different drugs and targets have different meta-paths. With the updating of model parameters, the vector representation of drugs and targets will be constantly updated, and then become completely different.

Although there are a large number of drugs and targets, the interaction between drugs and targets has rarely been verified. Aiming at this imbalance of data, we design experiments under different negative case ratios. We tested the positive and negative ratios of 1:1, 1:5 and 1:10, respectively, to verify the generalization ability of the model when the number of negative cases is much greater than that of positive cases. From the results in Table 6, we can see that even if the positive and negative examples are unbalanced, the results of AUROC and AUPR of our model are still very stable.

3.2.6 Robustness test

Finally, we conduct robustness test of our model. We try to find the positive DTI samples Δ with high homology following the strategies in Luo's paper: (i) DTIs involving homologous proteins (sequence recognition score > 40%); (ii) DTIs with similar drugs (Tanimoto coefficient > 60%); (iii) DTIs of which the drug had similar side effects (Jaccard similarity score > 60%); (iv) DTIs with drugs or proteins related to similar diseases (Jaccard similarity score > 60%); and (v) DTIs with similar drugs (Tanimoto coefficient > 60%) or homologous proteins (sequence consistency score > 40%).

Then we conduct the following experiments on Δ : (i) remove the positive DTI samples with high homology from the training set, and see if the model can predict these DTI interactions in the test phase; and (ii) use the positive DTI examples with high homology as negative examples in the training set, to see if the model can predict DTI interactions in the testing stage. In this way, we can simulate the false negative examples of

Table 7. Example of robustness test result in Luo's DTI data

Drug-Proteins	Result
Olanzapine—CHRM3	True
Olanzapine—DRD5	True
Olanzapine—CHRM5	True
Olanzapine—ADRA2C	True
Olanzapine—CHRM4	True
Olanzapine—HTR2C	True
Olanzapine—ADRA2B	True
Olanzapine—ADRA1B	True
Olanzapine—DRD3	True
Olanzapine—HTR1D	True
Accuracy	100%
Pergolide—DRD5	True
Pergolide—ADRA2C	True
Pergolide—HTR2C	True
Pergolide—ADRA2B	True
Pergolide—ADRA1B	True
Pergolide—DRD3	True
Pergolide—HTR1D	True
Pergolide—ADRA1D	True
Accuracy	100%

DTIs. For the first strategy, we successfully predicted 673 interactions out of 685 removed DTIs, with an accuracy of 98.2%, while the second strategy successfully predicted 606 interactions, with an accuracy of 88.5%. Through the above experiments, we find that our model is robust in the case of false negatives, and can still predict DTIs with high homology. We randomly selected two drugs and their related targets were predicted correctly, and showed the results in Table 7.

4 Discussion

In this article, we propose an end-to-end supervised graph co-contrastive learning model for the task of DTI prediction. Our model contrasts topology structures and semantic features of the DPP network and benefits from the valuable supervision information. We conduct comprehensive experiments and demonstrate significant improvements over competitive baselines on three public datasets. We also show that our proposed objective makes the model more robust, especially in the cold start scenarios.

Acknowledgement

The authors thank the anonymous reviewers for their constructive suggestions.

Funding

This work was supported by the National Natural Science Foundation of China [62072095, 61806049, 61771165]; and the Heilongjiang Postdoctoral Science Foundation [LBH-ZZ20104].

Conflict of Interest: none declared.

Data availability

Experimental datasets and experimental codes can be found in <https://github.com/catly/SGCL-DTI>.

References

- Cheng, F. *et al.* (2012) Prediction of drug–target interactions and drug repositioning via network-based inference. *PLoS Comput. Biol.*, **8**, e1002503.
- Ciortan, M. and DeFrance, M. (2021) Contrastive self-supervised clustering of scRNA-seq data. *BMC Bioinformatics*, **22**, 280.
- Feng, Y. *et al.* (2017) Drug target protein–protein interaction networks: a systematic perspective. *BioMed Res. Int.*, **2017**, 1289259.
- Fu, G. *et al.* (2016) Predicting drug target interactions using meta-path-based semantic network analysis. *BMC Bioinformatics*, **17**, 160.
- Gao, K.Y. *et al.* (2018) Interpretable drug target prediction using deep neural representation. In: Lang, J. (ed.) *Proceedings of the Twenty-Seventh International Joint Conference on Artificial Intelligence, IJCAI 2018, July 13–19, 2018, Stockholm, Sweden*, pp. 3371–3377. [ijcai.org](https://www.ijcai.org).
- Gong, J. *et al.* (2020) Attentional graph convolutional networks for knowledge concept recommendation in MOOCS in a heterogeneous view. In: Huang, J. *et al.* (eds.) *Proceedings of the 43rd International ACM SIGIR Conference on Research and Development in Information Retrieval, SIGIR 2020, Virtual Event, China, July 25–30, 2020*. ACM, pp. 79–88.
- González-Díaz, H. *et al.* (2011) Mind-best: web server for drugs and target discovery; design, synthesis, and assay of MAO-b inhibitors and theoretical-experimental study of G3PDH protein from *Trichomonas gallinae*. *J. Proteome Res.*, **10**, 1698–1718.
- Gunel, B. *et al.* (2021) Supervised contrastive learning for pre-trained language model fine-tuning. In: *9th International Conference on Learning Representations, ICLR 2021, Virtual Event, Austria, May 3–7, 2021*. <https://openreview.net/forum?id=cu7UioHujH>.
- Hafidi, H. *et al.* (2020) GRAPHCL: Contrastive Self-Supervised Learning of Graph Representations. *Advances in Neural Information Processing Systems 33: Annual Conference on Neural Information Processing Systems 2020, NeurIPS 2020, December 6–12, 2020, virtual*. 207–225.
- Iorio, F. *et al.* (2010) Discovery of drug mode of action and drug repositioning from transcriptional responses. *Proc. Natl. Acad. Sci. USA*, **107**, 14621–14626.
- Keiser, M.J. *et al.* (2007) Relating protein pharmacology by ligand chemistry. *Nat. Biotechnol.*, **25**, 197–206.
- Khosla, P. *et al.* (2020) Supervised contrastive learning. In: Larochelle, H. *et al.* (eds.) *Advances in Neural Information Processing Systems 33: Annual Conference on Neural Information Processing Systems 2020, NeurIPS 2020, December 6–12, 2020, virtual*. pp. 18661–18673.
- Kipf, T.N. and Welling, M. (2016) Semi-supervised classification with graph convolutional networks. *5th International Conference on Learning Representations, ICLR 2017, Toulon, France, April 24–26, 2017, Conference Track Proceedings*. pp. 1609–1616.
- Li, J. *et al.* (2021) Imchgan: inductive matrix completion with heterogeneous graph attention networks for drug–target interactions prediction. *IEEE/ACM Trans Comput Biol Bioinform.* 2021 Jun 11; doi: 10.1109/TCBB.2021.3088614.
- Luo, Y. *et al.* (2017) A network integration approach for drug–target interaction prediction and computational drug repositioning from heterogeneous information. *Nat. Commun.*, **8**, 1–13.
- Meng, F.-R. *et al.* (2017) Prediction of drug–target interaction networks from the integration of protein sequences and drug chemical structures. *Molecules*, **22**, 1119.
- Mizutani, S. *et al.* (2012) Relating drug–protein interaction network with drug side effects. *Bioinformatics*, **28**, i522–i528.
- Mongia, A. and Majumdar, A. (2020) Drug–target interaction prediction using multi graph regularized nuclear norm minimization. *PLoS One*, **15**, e0226484.
- Peng, J. *et al.* (2020) A learning-based method for drug–target interaction prediction based on feature representation learning and deep neural network. *BMC Bioinformatics*, **21**, 1–13.
- Peng, J. *et al.* (2021) An end-to-end heterogeneous graph representation learning-based framework for drug–target interaction prediction. *Brief. Bioinf.*, **22**, bbaa430.
- Shaikh, N. *et al.* (2016) An improved approach for predicting drug–target interaction: proteochemometrics to molecular docking. *Mol. Biosyst.*, **12**, 1006–1014.
- Sirota, M. *et al.* (2011) Discovery and preclinical validation of drug indications using compendia of public gene expression data. *Sci. Transl. Med.*, **3**, 96ra77.
- Sun, M. *et al.* (2020) Graph convolutional networks for computational drug development and discovery. *Brief. Bioinf.*, **21**, 919–935.
- Velickovic, P. *et al.* (2017) Graph Attention Networks. In: *6th International Conference on Learning Representations, {ICLR} 2018, Vancouver, BC, Canada, April 30 – May 3, 2018, Conference Track Proceedings*, pp. 1710–1718.
- Wang, W. *et al.* (2014) Drug repositioning by integrating target information through a heterogeneous network model. *Bioinformatics*, **30**, 2923–2930.
- Wang, X. *et al.* (2020) AM-GCN: adaptive multi-channel graph convolutional networks. In: *KDD '20: The 26th ACM SIGKDD Conference on Knowledge Discovery and Data Mining, Virtual Event, CA, USA, August 23–27, 2020*, pp. 1243–1253.
- Wang, X. *et al.* (2021a) Self-supervised heterogeneous graph neural network with co-contrastive learning. In: *Proceedings of the 27th ACM SIGKDD Conference on Knowledge Discovery and Data Mining, KDD '21, Association for Computing Machinery, New York, NY, USA*. pp. 1726–1736.
- Wang, Y. *et al.* (2021b) Multi-view graph contrastive representation learning for drug–drug interaction prediction. In: *WWW'21: The Web Conference 2021, Virtual Event / Ljubljana, Slovenia, April 19–23, 2021*, pp. 2921–2933.
- Wen, M. *et al.* (2017) Deep-learning-based drug–target interaction prediction. *J. Proteome Res.*, **16**, 1401–1409.
- Xia, Z. *et al.* (2010) Semi-supervised drug–protein interaction prediction from heterogeneous biological spaces. *BMC Syst. Biol.*, **4**, S6.
- Xue, H. *et al.* (2018) Review of drug repositioning approaches and resources. *Int. J. Biol. Sci.*, **14**, 1232–1244.
- Yamanishi, Y. *et al.* (2010) Drug–target interaction prediction from chemical, genomic and pharmacological data in an integrated framework. *Bioinformatics*, **26**, i246–i254.
- You, Y. *et al.* (2020) Graph Contrastive Learning with Augmentations. In: *Advances in Neural Information Processing Systems 33: Annual Conference on Neural Information Processing Systems 2020, NeurIPS 2020, December 6–12, 2020, virtual* **33**, 5812–5823.
- Zeng, X. *et al.* (2020) Target identification among known drugs by deep learning from heterogeneous networks. *Chem. Sci.*, **11**, 1775–1797.
- Zhao, T. *et al.* (2021) Identifying drug–target interactions based on graph convolutional network and deep neural network. *Brief. Bioinf.*, **22**, 2141–2150.
- Zheng, Y. *et al.* (2018) Predicting drug targets from heterogeneous spaces using anchor graph hashing and ensemble learning. In: *2018 International Joint Conference on Neural Networks, IJCNN 2018, Rio de Janeiro, Brazil, July 8–13, 2018*, (pp. 1–7). IEEE.
- Zhu, Y. *et al.* (2020) Graph Contrastive Learning with Adaptive Augmentation. In: *WWW'21: The Web Conference 2021, Virtual Event / Ljubljana, Slovenia, April 19–23, 2021* (pp. 2069–2080).